DLR-IB-SY-BS-2023-113

On measuring laminate strains of a bent tapered Double-Double panel – Comparing strain data from an FE calculation, a high-resolution 3D camera system (ARAMIS) and a fiber-optical sensor system (FOSS)

Wissenschaftlicher Bericht

Dr.-Ing. Erik Kappel
Yannick Boose
Robert Prussak
Jens Kosmann

Deutsches Zentrum
DLR für Luft- und Raumfahrt

Institut für Systemleichtbau

DLR-IB-SY-BS-2023-113

On measuring laminate strains of a bent tapered Double-Double panel – Comparing strain data from an FE calculation, a high-resolution 3D camera system (ARAMIS) and a fiber-optical sensor system (FOSS)

Zugänglichkeit:

Stufe 1 - Allgemein zugänglich: Der Interne Bericht wird elektronisch ohne Einschränkungen in ELIB abgelegt. Falls vorhanden, ist je ein gedrucktes Exemplar an die zuständige Standortbibliothek und an das zentrale Archiv abzugeben.

Braunschweig, *August, 2023*

Der Bericht umfasst: 31 Seiten

Abteilungsleiter:
Prof. Dr.-Ing. Christian Hühne

Autor:
Dr.-Ing. Erik Kappel

Autor 2 / Betreuer:
Yannick Boose
Robert Prussak
Jens Kosmann

Deutsches Zentrum für Luft- und Raumfahrt

On measuring laminate strains of a bent tapered Double-Double panel – Comparing strain data from an FE calculation, a high-resolution 3D camera system (ARAMIS) and a fiber-optical sensor system (FOSS)

Erik Kappel[a,*], Yannick Boose[a], Robert Prussak[a], Jens Kosmann[a]

[a] *DLR, Institute of Lightweight Systems (SY), Lilienthalplatz 7, 38108 Braunschweig, Germany*

Abstract

The article reports on a preliminary experimental study, which was executed to validate the laminate tapering approach for Double-Double (DD) laminates A cantilever scenario is examined, in which a defined vertical tip displacement is applied to a panel, whose shape is evaluated. Therefore, FE model predictions are compared with the real shape of correspondingly manufactured panels.

The second ambition of the study was to validate the strain output of a novel fiber-optical sensor system (FOSS). For this purpose, fiber-optical sensors were embedded during manufacturing in the tapered DD panel. Three fiber sensors were positioned at different locations within the tapered laminate stack. They provide continuous strain information along their entire length, with a resolution of approximately 0.6 mm. The 500 mm long panel has been subjected by a 50 mm tip displacement, while strain is evaluated along the bent. The panel's top-surface strain is additionally measured using a novel 24M GOM ARAMIS system. A comparison of the determined strain distributions from FE analysis (ABAQUS), FOSS and the optical measurement represents the core of the present article. Additional tests were executed to assess the strain data quality for different sensor-application approaches. Integrated and attached sensors are compared.

Keywords: Composite design, Double-Double laminate, Thickness tapering, Flex panel, Aero shape, Strain data

1. Motivation

The examined scenario is deduced from a future leading edge (LE) design. The CFRP components mimic a section of a full-scale panel, with one side being attached to the wing spar region, while the tip is linked to a slat kinematic. The outer surface of the CFRP component is exposed to airflow in the addressed reference application. The study examines the design task of tailoring the panel's shape for the bent case, by adapting the local CFRP layups and zone lengths.

* Tel.:+49 531 295 2398

Email address: erik.kappel@dlr.de (Erik Kappel)

Figure 1 shows the simplified test stand. It mimics the LE scenario with a 2.5D cantilever representation. The test stand allows for the application of a defined tip displacement to two CFRP panels. A tapered and a constant thickness panel have been manufactured.

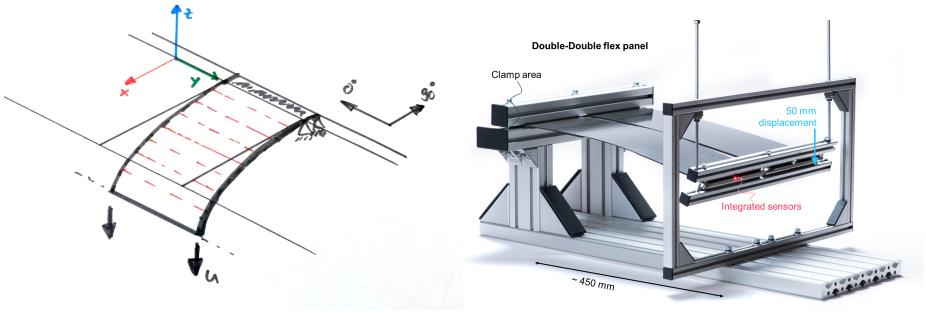

(a) Concept sketch (b) Created test setup

Figure 1: Object of investigation. Tip-displacement induced panel deflection

In a first study part (see [3] for details) a satisfying match between the deflection shape has been verified, by comparing outer surface's shapes, captured with a GOM ATOS system, with predictions of an corresponding FE model (ABAQUS).

The present article reports on the study's second perspective, which focuses on strain measurements using a novel fiber-optical-sensor-system (denoted as FOSS hereafter) and a recent GOM 24M ARAMIS system, which allows for surface strain measurements. In the study's second part, strain is evaluated for the described static tip displacement and results of both systems are compared with results of the corresponding FE analysis. The boundary conditions of the panels can be briefly described by

$$\begin{aligned} &w(x=0)=0 \\ &w(x=L)=u=50 \text{ mm} \\ &w(0<x<L)=f(\text{zone length, Laminate properties}) \quad . \end{aligned} \tag{1}$$

The CFRP parts feature Double-Double (DD) laminates [1], as those offer favourable tapering opportunities. As the tapered sample shows a more complex strain state, with severe strain inhomogeneity, the present article focuses on this configuration.

2. Double-Double laminate manufacturing

Local laminate thinning and thickening allows for tailoring a panels shape, when it is subjected by a tip displacement. The panel's local curvature can be altered, by adjusting individual laminate-zone lengths and the zone-specific thicknesses. The DD concept assures zone-to-zone compatibility, as all laminates are based on a pre-defined, balanced four-ply building block (BB). The panel's DD laminates feature a $[0, 50, -50, 0]$ building block, with the 0°-direction being aligned along the width direction (see Figure 1a) of the CFRP parts. The laminates are denoted as $[0, 50, -50, 0]_{rT}$, while the repeat parameter

r varies locally. The index T denotes 'total', which is in line with Nettles [9] and other publications on DD. The laminates are made from HEXCEL's M21E/IMA medium-grade, unidirectionally reinforced (UD) prepreg. The samples are cured in a $180°C$ autoclave process, using a single-sided tool concept and a conventional vacuum bagging setup. The nominal ply thickness is 0.184 mm. Thus, the laminate thickness varies from 1.47 mm up to 5.15 mm, referring to 8 ($r = 2$) up to 28 ($r = 7$) plies, respectively. Eight equi-length zones are defined along the panel length[1]. Figure 2 shows the local BB repeats. The red lines indicate the fiber sensors' locations within the laminate stack[2]. The dashed red line indicate a fiber sensor glued to the surface, which is later examined in Section 6. Dashed white lines indicate local neutral axes.

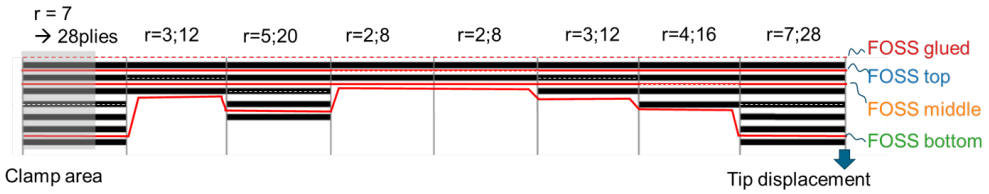

Figure 2: Fiber sensor positions in the tapered DD laminate. Thick black lines indicate a full four-ply building blocks

The first part of the experimental study[3] revealed a satisfying match between the measured (GOM ATOS scan) and the numerically predicted deformation, which is summarized in Figure 3.

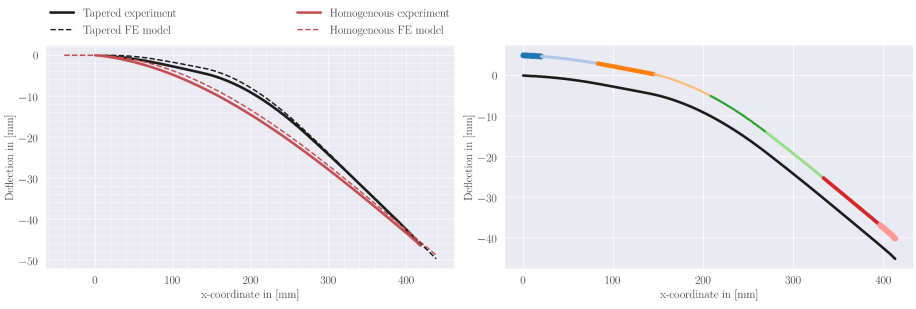

(a) Deflection (b) Tapering effect

Figure 3: Validation of the tapering opportunities. Colors and line thicknesses in the right plot indicate the zones and local material thickness

The study's second part focuses on determining strain in and on top of the tapered CFRP part with multiples fiber sensors and an optical system.

[1]Note that zone lengths can be adapted to further adjust the panels bent shape.

[2]Note, that the eight-zone configuration can be described in short based on the BB repeats [7,3,5,2,2,3,4,7] (from clamp-region to tip)

[3]A detailed report on the study's first part can be found in Tsai et al. [3].

Figure 4 shows the bottom surface of the tapered DD panel. The fibers shine red, which is realized using special illumination equipment for optical fibers.

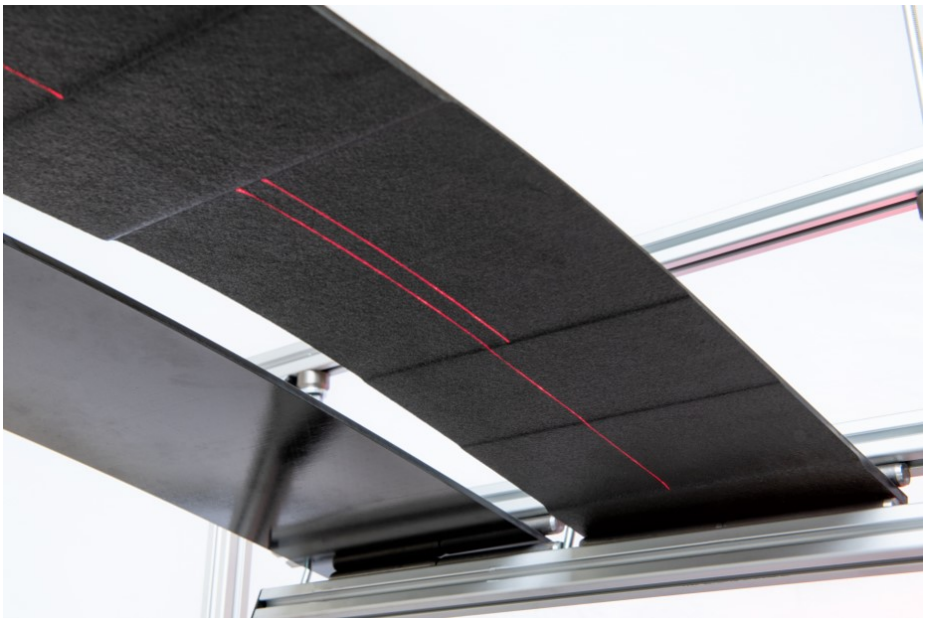

Figure 4: Bottom view on bent DD panel, with illuminated fiber sensors

It is important to highlight, that fibers are locally located on the part's outer surface, while in selected regions, fibers are located within the laminate stack. In those regions, the fibers is located in-between DD's building-blocks, which needs to be kept in mind for the strain comparison with FE data later on in the article.

3. FE models in ABAQUS CAE

FE representations of both panels have been created in ABAQUS CAE 6.14. The models mimics the bending scenarios, shown in Figure 1. The parts are modelled surface-based, with conventional four-node shell elements of type (S4). The tapered panel features eight zones, while the laminate in each zone is defined individually using the 'Composite Layup' functionality in ABAQUS. The following analysis focus on the tapered panel, as it provides a more challenging curvature profile and related strain discontinuities. The constant thickness panel is not further discussed on the present article, for sake of conciseness.

Figure 5 shows strains along the bent of the tapered panel for the bottom and the top-surface. Note, that Figure 5 also illustrates the local shell thickness (5x magnified). Due to the indicated scenario context, of an aerodynamically relevant surface, 'top-surface' modelling was executed. This is mandatory to assure a smooth outer surface, although laminate thicknesses differ. The selection is also linked to the manufacturing procedure, in which the whole laminate is cured on a flat tool, leading to a stepped bag-side surface of the part (see Figure 14).

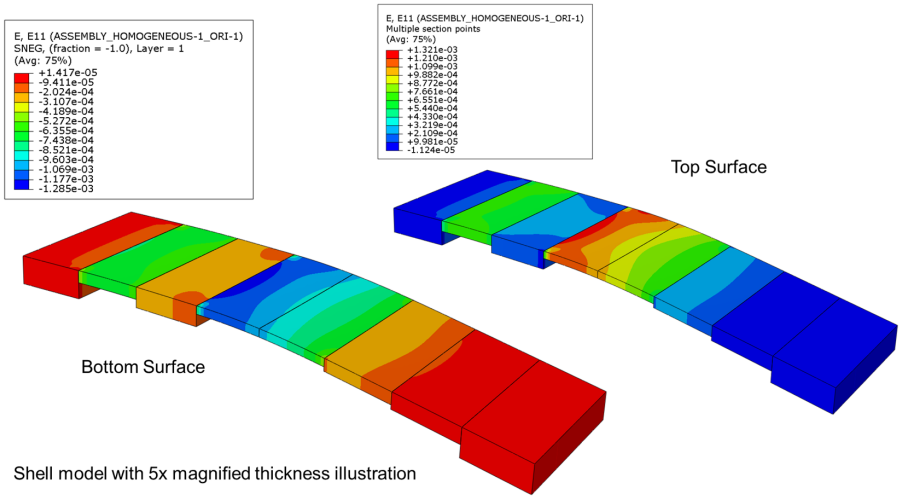

Figure 5: Top and bottom surface strain along bent. Shell-element model with illustrated local laminate thicknesses

Figure 6 summarizes the outer-surface strain for the top and the bottom surface, in the bent condition. The data is extracted for nodes along the symmetry plane (xz-plane in Figure 1a).

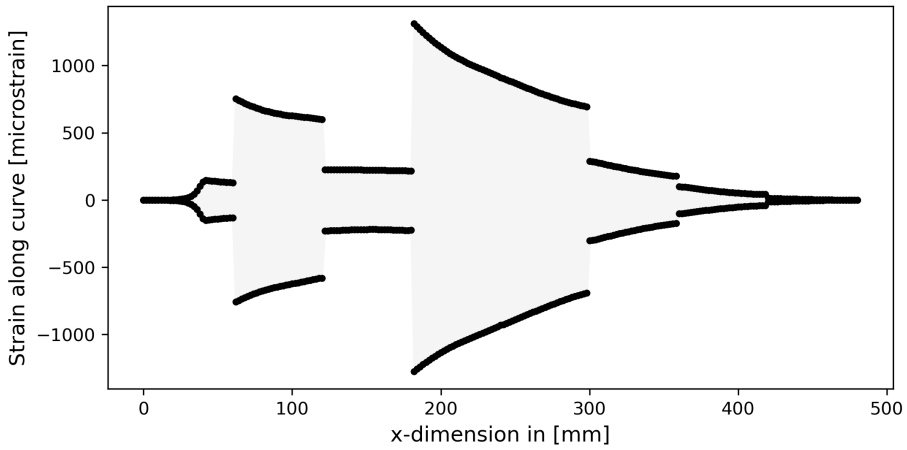

Figure 6: Top and bottom surface strain illustration along the bent panel

The local differences arise from locally different curvature ($\varkappa$) and laminate thicknesses t_{lam}.

$$\varepsilon_{max} = \varkappa \cdot \frac{t_{lam}}{2} \quad , \quad \varepsilon_{min} = -\varkappa \cdot \frac{t_{lam}}{2} \tag{2}$$

In contrast to strain gauges, fiber-optical sensors can be integrated in the laminate

stacking. In the present case, the sensors are locally positioned underneath the outer DD building block, as shown in Figure 2. Thus, the fibers measure strain inside the laminate and not on the outer surfaces. This must be accounted for when strains from the FE calculations are extracted for sake of comparison. Figure 7 shows the laminate built philosophy in ABAQUS and outlines how so-called section points are numbered.

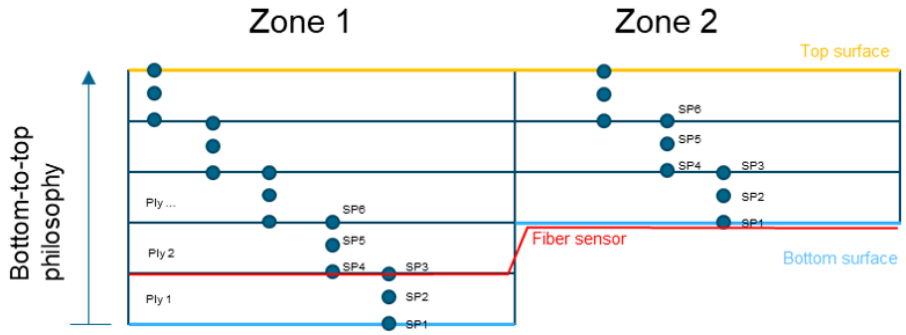

Figure 7: Section-point numbering concept for

In order to export the relevant strain information for zones of the tapered configuration, individual, zone-specific section-point selections need to be selected for the export [4]. Either SP3 or SP4 need to be selected for zone 1 and SP1 for zone 2, in order to compare FE-based strain with the fiber sensor data.

4. Strain measurement

As gravity impacts the deflection and therefore part strains, the strain measurement procedure needs to be defined accurately, to assure comparability between FE, FOSS and ARAMIS data. The study at hand focuses on the strain state for a static displacement. For the experiment, the panels are positions to the flat reference state first. This state is used to tare the strain data in the FOSS and the ARAMIS data. In the second step, the defined 50 mm displacement is adjusted by using the threaded rods of the test stand. The deflection is adjusted precisely and fixed using clamps. Strain data is captured for the bent state. Due to the tare operation, strain of all three sources FE, FOSS and ARAMIS become comparable [5].

FOSS measurement

A LUNA ODiSI 610X Optical Distributed Sensor Interrogator [10] has been used for the test. Figure 8 shows the FOSS infrastructure during the measurement.

[4] Section point outputs need to be requested in the ABAQUS input file, as top- and bottom-surface strains are stored only, as the standard.

[5] Note, that gravity effects are not considered in the FE model.

Figure 8: FOSS system during the measurement. Test stand in background

GOM Aramis measurement

A GOM 24M ARAMIS system [11] has been used, for the optical strain measurements. Figure 9 shows the test setup in deflected state during the data capturing procedure. Figure 9b shows an overlay of the sensor's camera image and the captured strain information, which is shown in detail in Figure 10.

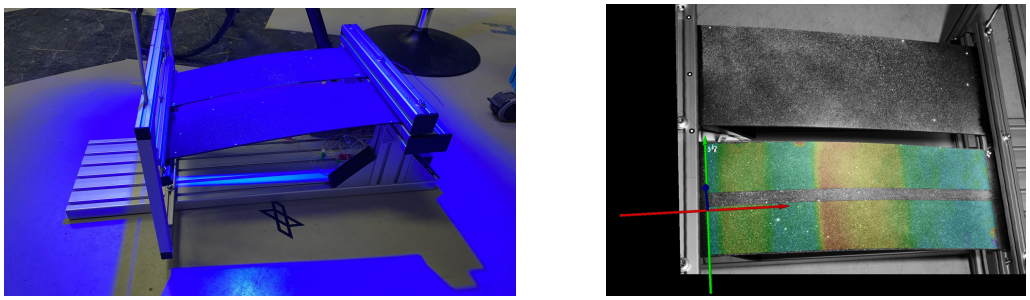

(a) During (b) strain on tapered panel (see Figure 10)

Figure 9: ARAMIS measurement and strain data on tapered panel

Note, that the white region in Figure 10 has been removed from the strain evaluation (see also Figure 9b). In this region, additional fibers have been attached to the panel as an approach to measure surface strain (see Section 6 above). The corresponding surface disturbance impedes the optical strain evaluation, which led to the removal.

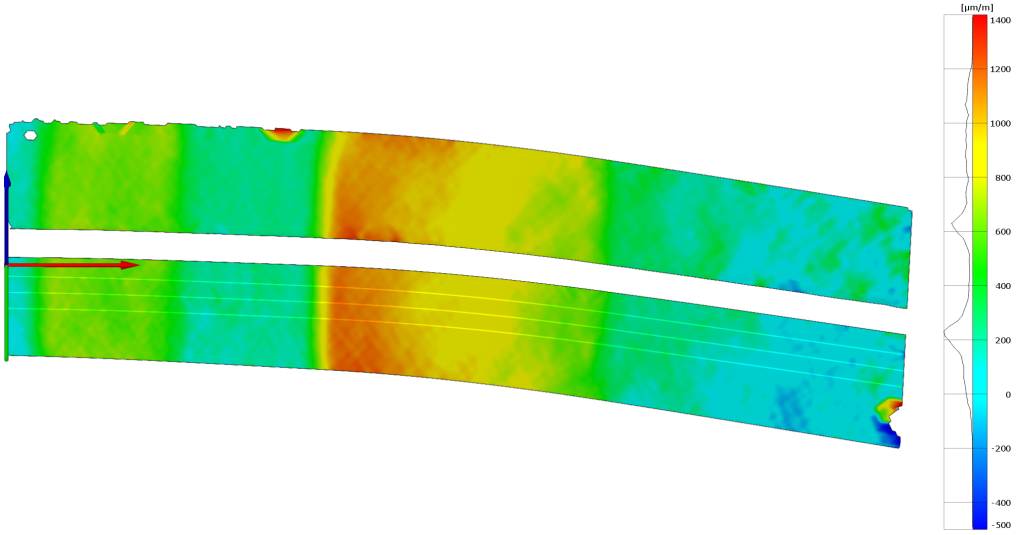

Figure 10: ARAMIS strain data with three defined sections defined for local strain assessment

Strain has been evaluated along three parallel sections, which can be seen in Figure 10, As not relevant deviation was observed, only a single data set is further used hereafter. The legend, shown in Figure 10, covers a rage from -500 up to 1400 microstrain, which deviates from the strain values plotted in Figure 5. Figure 11 shows top-surface FE result, while legend has been adapted to the range of the ARAMIS plot, with the strain being illustrated in microstrain.

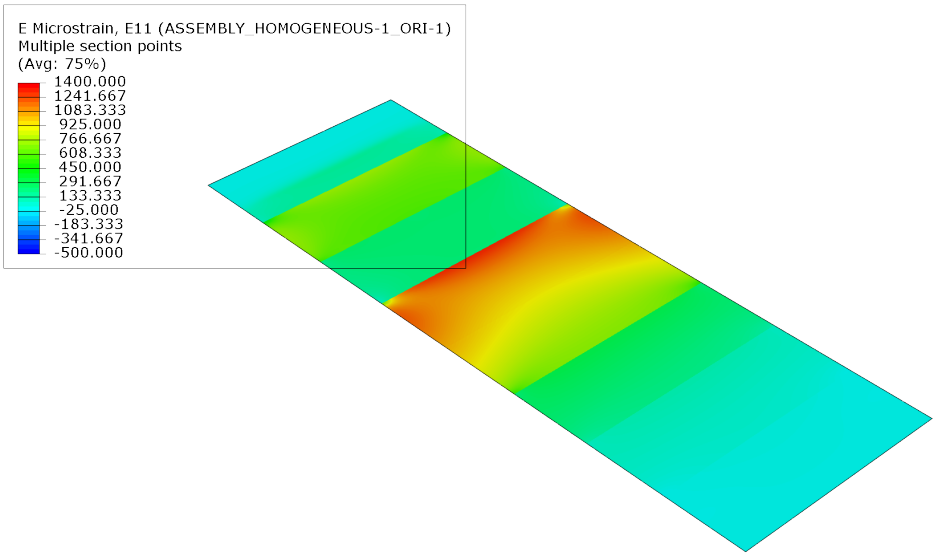

Figure 11: FE result, with legend adapted to GOM output in Figure 10, with a strain range from -500 to 1400 to microstrain

5. Results

The results of the individual data strain-data sources are examined hereafter in common plots. The plots feature:

- Top- and bottom-surface strain from the FE model
- 'In-laminate' Strain from FE model, extracted for the actual location of the bottommost optical fiber in the stack
- Strain data for top-surface, captured with the GOM ARAMIS system
- Strain data of an optical fiber fully glued to the outer surface of the tapered panel (FOSS)
- Strain data of three embedded fibers (FOSS)

Note, that 'horizontal' data alignment is mandatory to realize meaningful plots. While FE data is available for the entire part length, optical data of the ARAMIS measurement is determined beyond the clamping area. Similarly, the FOSS data has been extracted for the same region only. The alignment has been realized by manual adjusting the x-coordinates of the different data sets. Strain magnitudes were not modified, despite a transfer to 'microstrain'. Figure 12 summarizes FOSS data sets.

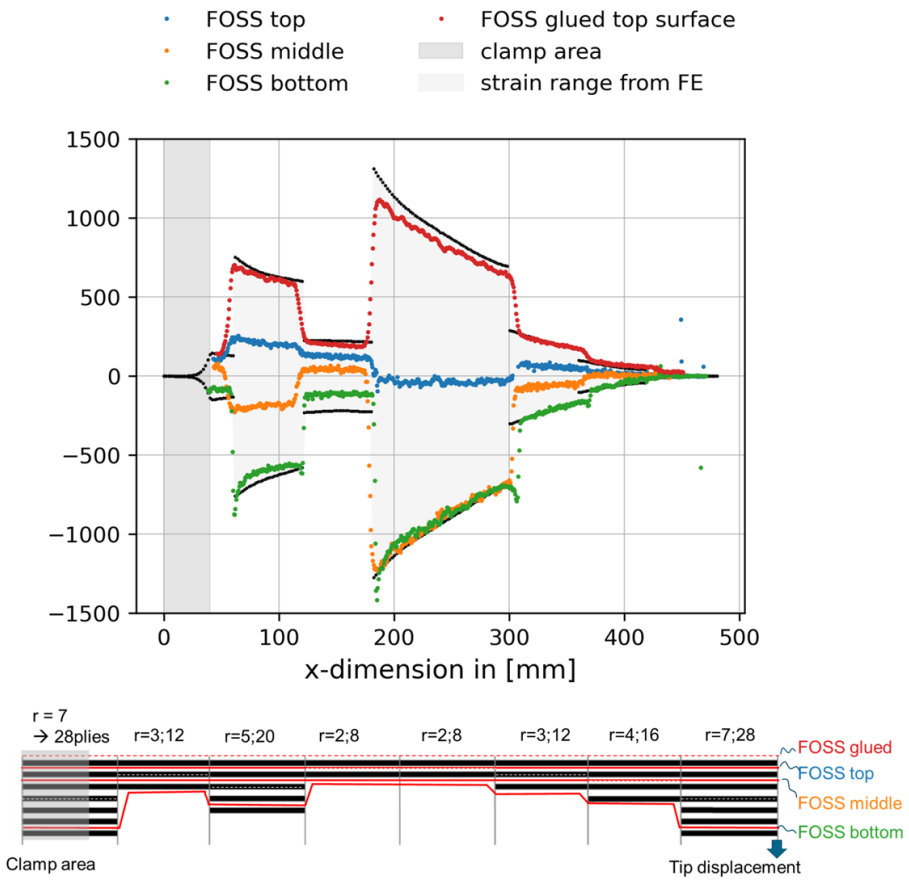

Figure 12: Measured FOSS data sets for the integrated and a single externally attached fiber

The plot shows the unique FOSS capability of capturing continuous strain data along a part, while positioning multiple fibers at different positions of the laminate thickness additionally allows for assessing through-the-thickness strain distributions. Strain gauges, for example, provide a single local strain value on the part surface. Fiber-Braggs also provide a single strain information at the Bragg-grating location (multiple Bragg-grating in a single fiber possible) from within a laminate. The ARAMIS system provides continuous strain data as well, but it's application is limited to outer-surface strains an accessibility is mandatory to perform scans.

Figure 13 summarizes the results of the executed experiment. The left portion of Figure 13 shows the top surface result. As the uppermost integrated fiber was positioned underneath the uppermost BB, the generated strain data cannot be directly compared with top-surface data from FE and the ARAMIS measurement. Thus, FOSS strain data from of an fiber fully glued to the top surface, is plotted.

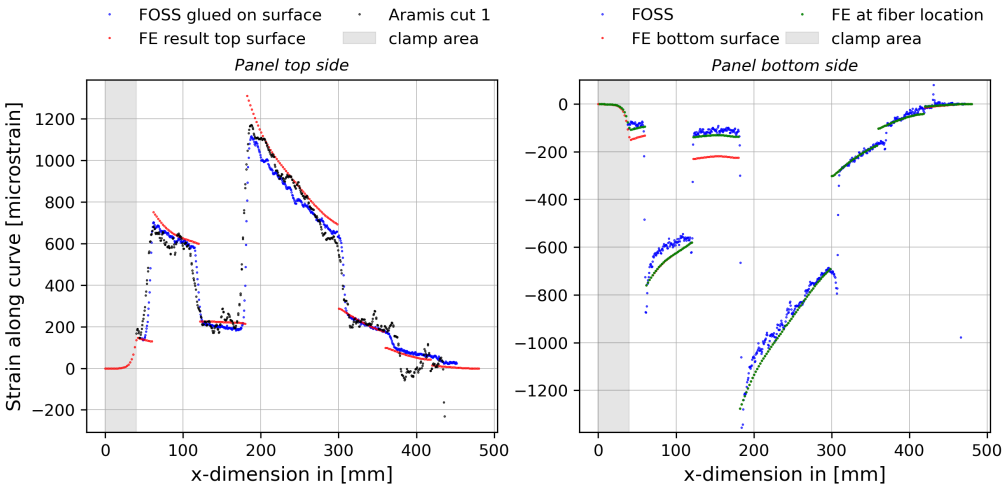

Figure 13: Top-surface and bottom-surface results at a glance. (red) FE surface strains, (blue) FOSS strain results, (black) ARAMIS strain results, (green) FE in-laminate strains at fiber location

The right part of Figure 13 shows the strain for the bottom surface and the bottommost fiber in the laminate stack. Due to limited accessibility no ARAMIS data was generated for the bottom side.

Both measurement technique capture the discontinuous strain along the tapered panel excellently. The FE data sets show discrete steps in the strain graphs. Those, are a consequence of the shell-element modelling, which feature discrete thickness steps at zone-to-zone transitions. The tapered panel has been manufactured with a single-sided tool concept. The vacuum bag, at the part's inner surface, always leads to slight smothering of the local thickness changes due to local variation of BB repeats. Figure 14 indicates the difference between FE idealization of zones and the parts real shape after the manufacturing process.

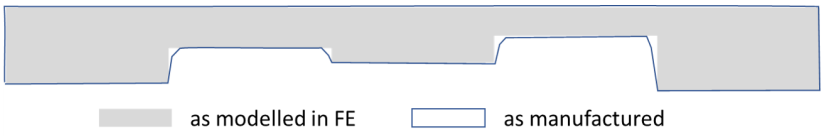

Figure 14: FE idealization versus manufactured reality

As the fibers run through those regions, they will always provide local strain information, in between the discrete levels of the FE data. Nonetheless, it is concluded that the comparison substantiate that both measurement approaches provide high-resolution strain information, which meets corresponding FE result excellently in terms of magnitude and also in terms of local distribution. The examined cantilever scenario, with 50 mm tip displacement, leads to a strain maximum of 1311 microstrain on the top surface, located at the transition from zone 3 to zone 4. A maximum compressive strain of -1276 microstrain is observed on the bottom surface at the same location.

6. Fiber integration vs. application

Integrating fiber sensors in composite laminates, in high-temperature autoclave processes can potentially been considered to impede process robustness. Exchanging a damaged fiber in a cured composite structure is hardly possible in addition. Thus, it can be a show stopper when important systems, as for example a flight-control-computer or a health monitoring system, need strain data from the integrated fibers as inputs.

Therefore, attaching sensors after a part has been made according to a conventional series process, is an important scenario for industrial applications. Existing, approved processes remain unaffected and robust. Neither modified processes nor new materials need to be qualified. In case of a sensor damage, accessibility is given, allowing for a sensor exchange or for attaching a new sensor to the structure.

The question *'Does an attached sensor provide the same insight and data quality as embedded sensors?'* needs to be answered. The tapered DD panel has been used to examine this aspect by executing three tests.

1. Attaching a sensor on the top surface using a industry scotch tape
2. Attaching a sensor using a 2k epoxy glue, while the sensor is glued completely along its length
3. Attaching a sensor locally using the same 2k epoxy glue, while 5 mm long sections are skipped in high-strain areas

Figure 15 replots the top-surface result from Figure 13, while a data set from a sensor attached with scotch-tape is added.

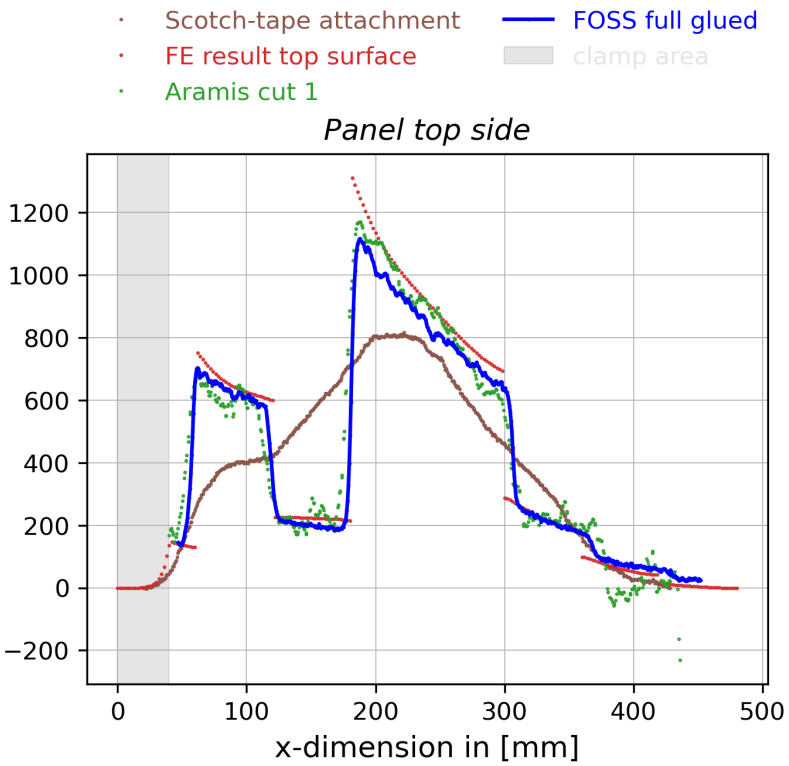

Figure 15: Top-surface strain. FE data, FOSS data from fully glued fiber, ARAMIS Data, and FOSS data from fiber attached with scotch tape

The novel data set also shows low and high-strain areas, which roughly follow the FE data. However, neither magnitudes nor local strain profiles are met satisfactorily. This leads to the conclusion that scotch-tape attachment does not provide useful data. In contrast, the fully-glued fiber provides high-quality results in terms of magnitude an local distribution. Thus, gluing the fiber along its entire length is considered the baseline solution, in order to receive adequate strain data. However, accessibility is not always given along the fiber's entire length, which leads the question *'What happens when fibers are discontinuously bonded to the panel in areas with strain discontinuities?'*,

Fully vs. locally glued fiber

An additional measurement was executed to answer the previous question. For this purpose, a second fiber has been attached to the panel's outer surface, parallel to the fully glued fiber. The additional fiber has been discontinuously attached to the panel. At zone-to-zone transitions, where surface-strain discontinuities are observed, the fiber remains unattached along 5 mm, as it can be seen in Figure 16a.

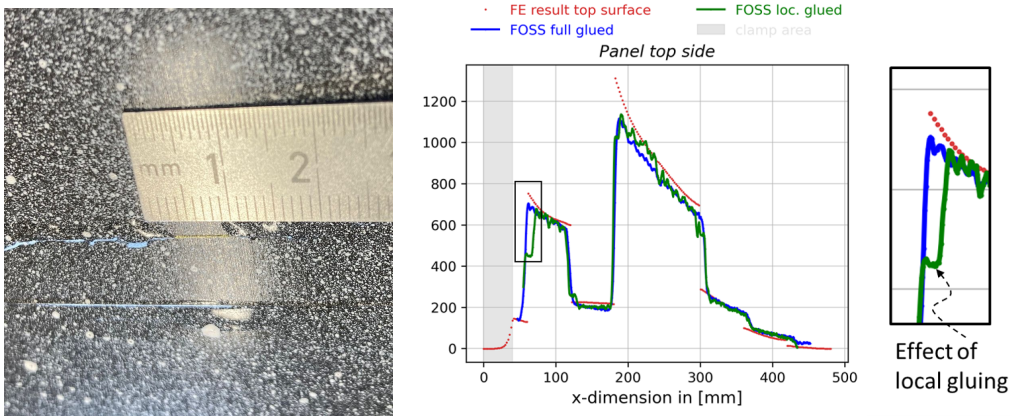

(a) Fiber locally unglued (5 mm)

(b) Measured strains

Figure 16: FOSS strain from locally and fully glued fibers on top surface

The captured strain data for the fully and the locally glued fibers is shown in Figure 16b. The excerpt in Figure 16b highlights the consequence to the strain data. It can be clearly seen that local steps in the strain signal are observed in regions, where the fiber is unattached. The situation is considered even more critical in a compression load scenario, as the thin fiber can buckle.

Thus, the simple test suggests the conclusion that a continuous attachment, along the full fiber length, is required to fully profit from the FOSS potentials. Locally attaching the fiber only is accompanied by the risk of not capturing potentially critical high-strain areas.

7. Conclusions & Outlook

The strain distribution of a tapered composite laminate has been examined and quantified experimentally. The carbon-fiber-epoxy laminates pursue the Double-Double philosophy, which provides excellent tapering options. A cantilever scenario test stand has been used, to subject the panels by a defined vertical tip displacement of 50 mm. The tapered laminate thickness induced a significant curvature inhomogeneity, while those result in discontinuities of the strain distribution along the bent panel. The measurement of the particular strain distribution is the main focus of the present article. Results of an FE simulation are compared with experimental data, captured with a LUNA FOSS system and a GOM ARAMIS optical measurement system. Fiber sensors were embedded in the DD laminate and externally attached to a panel's outer surface. The following list summarizes the outcomes of the conducted study.

- The severe strain inhomogeneity is well covered with both the LUNA FOSS and the GOM ARAMIS measurement systems. A convincing match with FE data is identified.
- An excellent match between FE and FOSS strains is observed, and the effect of the fiber position within the laminate stack can be clearly identified

- FE strain data shows discrete steps between the individual zones. FOSS and ARAMIS data both approximate those steps, with intermittent values being present. The effect is related to the FE model idealization, featuring step-like thickness changes and the manufactured samples, which feature slightly smoothed transitions due to the vacuum bag arrangement.
- Comparing FE data with embedded-fiber data requires particular care, as section-point data needs to exported zone specifically, in order to account for the fibers actual position in the laminate stack.
- In order to capture strain inhomogeneity along a part's length a simple test suggests that the fibers need to be attached to the part by an appropriate glue (2K epoxy for example) long their full length.
- Scotch-tape based attachment as well as local gluing detrimentally affects the strain data quality. The former approach even leads to hardly relevant strain information.

The executed study clearly demonstrates the capabilities of both sensor systems. Both systems provide high-resolution strain information, which match corresponding FE data in terms of magnitude and local distribution well. The high resolution is particularly valuable, as it allows for the analysis of inhomogeneous strain distributions with a single fiber or a single optical scan. The FOSS technology additionally offers the feature to measured strain inside the composite laminate stack, allowing for the analysis the through-thickness strain distributions.

Acknowledgments

The project '101101974 - UP Wing' is supported by the Clean Aviation Joint Undertaking and its members.

Disclaimer

Funded by the European Union. Views and opinions expressed are however those of the author only and do not necessarily reflect those of the European Union or Clean Aviation Joint Undertaking. Neither the European Union nor the granting authority can be held responsible for them.

CRediT author contribution statement

- Yannick: Sample manufacturing, FOSS data generation, illustration, reviewing
- Robert: FOSS data generation, illustration, reviewing
- Jens: ARAMIS data generation and evaluation
- Erik: Study concept development, data evaluation, illustration, writing

Declaration of competing interest

The authors declare that they have no known competing financial interests or personal relationships that could have appeared to influence the work reported in this paper.

[1] Tsai SW. Double-Double: New Family of Composite Laminates. AIAA Journal (https://doi.org/10.2514/1.J060659), 2021

[2] Tsai SW et al. DOUBLE-DOUBLE - A New Perspective in The Manufacture and Design of Composites. Composites Design Group. Stanford University, Stanford, CA 94305-4035, 2022

[3] Tsai SW et al. DOUBLE-DOUBLE Simplifying the Design and Manufacture of Composite Laminates. -Chapter 13- ICCM23 Belfast publication, July 2023

[4] Cunha RDd et al. Low velocity impact response of non-traditional double-double laminates. Journal of Composite Materials Vol. 0(0) 1-11, 2023

[5] Kappel E. Double-Double laminates for aerospace applications - Finding best laminates for given load sets. Composites Part C: Open Access 8, 100244, 2022

[6] Kappel E. Buckling of Double-Double laminates. Composites Part C: Open Access (submitted for publication) 2023

[7] HEXCEL M21 Data sheet. HexPly M21 180°C (350°F) curing epoxy matrix, 2020

[8] Talreja R, Modeling Damage, Fatigue and Failure of Composite Materials, Cambridge: Elsevier Science. Woodhead Publishing Series in Composites Science and Engineering, 2015

[9] Nettles AT, Basic Mechanics of Laminated Composite Plates - NASA Reference Publication 1351, Technical Report, NASA, 1994.

[10] LUNA. ODiSI 6000 Series Optical Distributed Sensor Interrogators. Data Sheet. https://lunainc.com/product/odisi-6000-series, 2023

[11] ZEISS ARAMIS 24M. https://www.gom.com/de-de/produkte/3d-testing/zeiss-aramis-adjustable-24m, 2023